Scientia Iranica B (2013) 20(4), 1228–1240

SCIENTIA IRANICA

Sharif University of Technology
Scientia Iranica
Transactions B: Mechanical Engineering
www.scientiairanica.com

Detailed investigation of hydrodynamics and thermal behavior of nano/micro shear driven flow using DSMC

O. Ejtehadi[a], E. Roohi[a,*] and J. Abolfazli Esfahani[a,b]

a. *Department of Mechanical Engineering, Faculty of Engineering, Ferdowsi University of Mashhad, Mashhad, P.O. Box: 91775-1111, Iran.*
b. *Center of Excellence on Modeling and Control Systems, Ferdowsi University of Mashhad, Mashhad, P.O. Box: 91775-111, Iran.*

Received 9 April 2012; received in revised form 6 February 2013; accepted 21 April 2013

KEYWORDS
DSMC;
Mon/diatomic gases;
Nano/micro Couette flow;
Knudsen layer;
Compressibility effects;
Rarefaction effects.

Abstract. In the present work, we simulate rarefied gas flow between two moving nano/micro parallel plates maintained at the same uniform temperature using the direct simulation Monte Carlo (DSMC) method. We perform simulations for monatomic argon and diatomic nitrogen gas and compare mon/diatomic gas behavior. For both gases, we study heat transfer and shear stress and investigate the effects of compressibility and rarefaction in the entire Knudsen regime and for a wide range of wall Mach numbers. Slip velocity, temperature jump, wall heat flux and wall shear stress are directly sampled from the particles striking the surfaces and reported for monatomic and diatomic cases for different rarefaction regimes. We also study deviation from the equilibrium using the probability density function for argon and nitrogen gas molecules.

1. Introduction

Micro/nanochannels are widely encountered in micro/nanoelectromechanical systems (MEMS/NEMS). To enhance the design and performance of such systems, it is necessary to achieve a deeper understanding of their flow and heat transfer behavior. When the Knudsen number is sufficiently large, the fluid rarefaction is the main parameter to evaluate these systems [1]. The degree of rarefaction is measured in terms of the Knudsen number (Kn). The Knudsen number is defined as the ratio of mean free path of a molecule to a characteristic length of the flow. Flow regimes are also classified on the basis of the Knudsen number into continuum (Kn$\leq$0.001), slip flow (0.001<Kn<0.1), transition flow (0.1<Kn<10) and free molecular (Kn$\geq$10) regimes.

When there is a continuum breakdown, the solutions are to be established based on kinetic principles such as those in treating the Boltzmann equation. However, deterministic methods based on the Boltzmann equation are complex and, hence, have motivated the development and application of the direct simulation Monte Carlo (DSMC) [2] method, which can also be regarded as a statistical method for the solution of the Boltzmann equation. The DSMC method possesses many advantages, such as simplicity of application, unconditional stability, and ease of modeling complex physical flows. However, the computational cost is larger than traditional computational fluid dynamics (CFD) approaches.

Shear-driven flow, such as Couette, are encountered in micro-motors, comb mechanisms and microbearings. In this study, we choose the well-known problem of planar Couette flow. Despite its simplicity, Couette flow includes many features found in complex rarefied gas dynamics problems. Micro-Couette flow, i.e. a gas confined between two infinite parallel plates which are at the same temperature but moving relative to each other, has been widely studied. For example Willis [3] used Krook's kinetic model to investigate

*. *Corresponding author. Tel: +98 511 8763304*
E-mail address: e.roohi@ferdowsi.um.ac.ir (E. Roohi)

Couette flow at low Mach numbers. He showed that velocity and shear stress could be calculated from the solution of an integral equation for the macroscopic velocity. He derived a slip boundary condition for Maxwell molecules and compared the derived solution with those of other moment-based kinetic models. Sirovich [4] developed an approximate method in kinetic theory for Couette flow and found expressions for slip coefficients as a function of degree of specular and diffuse reflections. The method was especially accurate for near-continuum flows. A slip coefficient within 1.5% of the exact value for purely diffuse reflection was calculated by this method. Beskok et al. [5] gave an analysis of the effects of compressibility and rarefaction on pressure-driven and shear-driven microflow. They found that compressibility and rarefaction are competing phenomena and both require consideration in microfluidic analysis. Marques et al. [6] investigated gaseous micro-Couette flow with the NS equations and compared results with the DSMC method in continuum and transition regimes. Their comparison between NS and DSMC solutions for the heat flux vector perpendicular to the plates showed that slip and jump boundary conditions are also important in the transition regime and do not necessarily depend on the velocities of the plates. Xue et al. [7-9] analyzed the micro-Couette flow using the DSMC method, the NS equations, and the Burnett equations, and found that rarefaction has a significant effect on velocity, temperature and pressure, especially for high Knudsen numbers. They stated that the non-dimensional parameter Prandtl-Ekcert (PrEc), characterizing convective heat transfer in Couette flow, increases as flow becomes more rarefied. Their prediction of shear stress and heat flux at the wall showed the superiority of Burnett equations over the NS equations in the micro-Couette flow simulations. Meanwhile, the Burnett equations with the slip boundary condition, which is proportional to the Knudsen number, cannot be extended to the transition flow regime. Frezzotti and Gibelli [10] proposed a kinetic model of fluid-wall interaction by simple extension of the Enskog theory of dense fluids, and applied the model to the case of thermal Couette flow. They also investigated the interaction of a dilute monatomic gas with a solid surface, compared Molecular Dynamics (MD) simulations with numerical solutions of the proposed kinetic model and showed that the results of the two simulations are close. In an another attempt, Frezzotti et al. [11] used their proposed fluid-wall interaction kinetic model to study the heat transport between parallel walls and Couette flow, and compared their results with MD simulations. The distribution functions of reemitted molecules and the accommodation coefficients obtained from the two techniques are compared, and it is shown that the kinetic model predictions are close to MD results. More recently, Frezzotti et al. [12] proposed a moment method based on the linearized Bhatnagar-Gross-Krook (BGK) kinetic model equation and applied the method to the cases of Couette, Poiseuille and cavity flow. Their results showed that excellent approximations of exact solutions of the kinetic model equation could be obtained using a small number of moments equations. Gu et al. [13] compared the DSMC solution of the Couette flow with a high order moment approach, i.e. 26 moment equations for capturing non-equilibrium phenomena in the transition regime. Their new set of equations overcame many of the limitations observed in the regularized 13 moment equations. Kumar et al. [14] investigated the accuracy of the statistical BGK and ellipsoidal statistical BGK (ESBGK) equations in comparison with the DSMC solution in the Couette flow. They showed that these methods are more efficient than the DSMC method for a flow condition that is at the comfort-level limit for direct simulation Monte Carlo computations.

The objective of the present work is to provide a deeper understanding of shear driven flow in micro/nano scale channels. Although simulation of Couette flow has been implemented before, the specific contribution of this work is a detailed comparison of the behavior of monatomic argon and diatomic nitrogen fluids, which is not reported in the literature. For both gases, we investigated important engineering parameters like heat flux and shear stresses, as well as compressibility and rarefaction effects over a wide range of Knudsen and Mach numbers. Slip velocity, temperature jump, wall heat flux and shear stress are directly sampled from particles impinging the walls and are reported for both gases. The approximate solutions for planar Couette flow are available within the framework of continuum fluid mechanics subject to velocity slip and temperature jump boundary conditions and valid for the low-velocity (subsonic) and low Knudsen number (Kn$\leq$0.1) flows [1,6,15]. Consequently, we compare our DSMC temperature, velocity, shear stress and heat flux profile with the approximate derivation at low Kn/Mach numbers. We also study deviation from the Maxwellian equilibrium distribution using the velocity distribution function of gas particles for both argon and nitrogen.

2. Present numerical analysis

2.1. Problem statement

Planar Couette flow involves one dimensional flow through a channel comprising two parallel plates at $y = \pm h/2$ moving relative to each other, with a constant velocity, $\pm U_w$, and maintained at the same temperature. It is depicted in Figure 1 schematically. The flow velocity is assumed to have only an axial component varying only in the y direction, and the external forces are assumed to be absent.

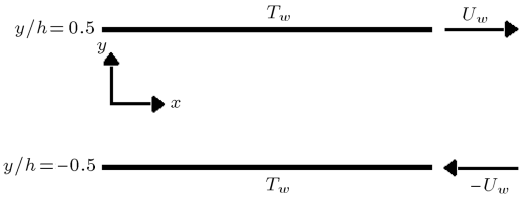

Figure 1. Schematic of the Couette flow.

2.2. The DSMC method

DSMC is a numerical tool to solve the Boltzmann equation based on direct statistical simulation of the molecular processes described by the kinetic theory [2]. It is considered a particle method, in which a particle represents a large bulk of real gas molecules. The primary principle of DSMC is to decouple the motion and collision of particles during one time step. The implementation of DSMC requires that the computational domain be broken down into a collection of grid cells. The cells are divided into subcells in each direction, and the subcells are then utilized to facilitate the selection of collision pairs. After fulfilling all molecular movements in the domain, the collisions between molecules are simulated in each cell, separately. In the current study, a variable hard sphere (VHS) collision model is used and the collision pair is chosen based on the no time counter (NTC) method. The channel walls are treated as diffuse reflectors using the full momentum/thermal accommodation coefficient. A full momentum accommodation coefficient means that the tangential momentum of reflected molecules is equal to the tangential momentum of the wall. Similarly, full thermal accommodation means that the energy flux of reflected molecules is equal to the energy flux corresponding to the wall temperature. The velocity of the reflected molecules ($\mathbf{c}'$) is randomly assigned according to the full thermal and momentum accommodation and a half-range Maxwellian distribution determined by the wall temperature [16] as follows:

$$\mathbf{c}'_x = \sqrt{-\log(RF(0))}V_{mpf}\sin(2\pi\cdot RF(0)), \tag{1}$$

$$\mathbf{c}'_y = \pm\sqrt{-\log(RF(0))}V_{mpf}, \tag{2}$$

$$\mathbf{c}'_z = \sqrt{-\log(RF(0))}V_{mpf}\cos(2\pi\cdot RF(0)). \tag{3}$$

where $V_{mpf} = \sqrt{2RT}$ is the most probable speed of the molecules at wall temperature and $RF(0)$ is a uniformly distributed random fraction between 0 and 1. The positive and negative symbols correspond to the lower and upper walls, respectively, and R is the gas constant.

An accurate DSMC solution requires some constraints on the cell size, time step and number of particles. The random selection of the particles from a cell for binary collisions requires the cell size to be a small fraction of the gas mean free path. The decoupling between the particles movements and collisions is correct if the time step is a small fraction of the mean collision time. The number of particles per cell should be high enough, around 20, to avoid repeated binary collisions between the same particles. The following procedure is used to solve a stationary problem with DSMC. In the entire computational domain, an arbitrary initial state of gas particles is specified and the desired boundary conditions are imposed at time zero. Particle movement and binary collisions are performed separately. After achieving steady flow condition, sampling of molecular properties within each cell is fulfilled during a sufficient time period to avoid statistical scattering. All thermodynamic parameters, such as temperature, velocity, density and pressure, are then determined from this time-averaged data. More details on the DSMC algorithm are given in [2,17].

3. Results and discussion

To simulate micro/nano-Couette flow, we modified the DSMC code used by Roohi and coworkers for simulation of different geometries, like micronozzle, microchannel, micro-cavity, and backward facing step [18-22]. In all simulations, monatomic argon and diatomic nitrogen gases are considered at a reference temperature of $T_{\text{ref}} = 273$ K with a reference dynamic viscosity of $\mu_{\text{Ar}} = 2.117\times10^{-5}$ Ns/m^2 and $\mu_{N_2} = 1.656\times10^{-5}$ Ns/m^2, respectively [2]. We considered argon gas with molecular mass of $m = 6.63\times10^{-26}$ kg, viscosity temperature index of $\omega = 0.81$ and variable hard-sphere diameter of $d_{\text{VHS}} = 4.17\times10^{-10}$ m, and nitrogen gas with molecular mass of $m = 4.65\times10^{-26}$ kg, viscosity temperature index of $\omega = 0.74$ and variable hard-sphere diameter of $d_{\text{VHS}} = 4.11\times10^{-10}$ m. The walls are set to have equal temperature of $T_w = 273$ K. Our simulations are performed for a wide range of Knudsen, varying from 0.01 to 10, and Mach numbers ranging from 0.2 to 1.2, and both compressibility and rarefaction effects, besides comparison of monatomic and diatomic molecule behavior, are investigated.

The macroscopic properties of interest in the paper are derived using molecular gas dynamics relations [2]. The viscous stress tensor, $\boldsymbol{\tau}$, is defined as the negative of the pressure tensor with the static pressure subtracted from the normal components.

$$\boldsymbol{\tau}_{ij} = -(\rho\overline{c_i c_j} - \boldsymbol{\delta}_{ij}p), \tag{4}$$

where c_i and c_j are the components of $\mathbf{c}$, the velocity of the molecule relative to stream velocity, called thermal velocity, and p is the scalar pressure defined as:

$$p = \frac{1}{3\varrho\overline{c^2}}. \tag{5}$$

The heat flux vector is defined as:

$$\mathbf{q} = 1/2\varrho\overline{c^2 c} + n\overline{\varepsilon_{int} c}, \tag{6}$$

where ε_{int} is the internal energy of a single molecule.

In figures, the ordinate is normalized by the distance between the parallel plates, h. Flow velocity and temperature are normalized by the relative velocity of the plates, U_w, and the temperature of the wall, T_w, respectively. Also, heat flux and shear stress are normalized by the parameters, $\rho_\infty U_w C_p T_w$ and $\frac{1}{2}\rho_\infty U_w^2$, respectively. Here, ρ_∞ and C_p are the free stream density and the specific heat capacity, respectively. The normalized heat flux and shear stress are referred to as the heat flux coefficient, C_h, and the friction coefficient, C_f, respectively, in the figures. Also, because of the symmetry in the upper and lower parts of the channel, in figures which include mon/diatomic comparison, we only report the solution for the upper half of the domain. We also calculated the velocity slip, temperature jump, heat flux and shear stress on the wall, based on the particles that strike the plates in the DSMC code, and compared the results with the macroscopic amounts near the plates. Slip velocity and temperature jump are defined as follows [23]:

$$U_{\text{slip}} = \frac{\sum\left(\left(m/\left|c_j\right|\right)c_i\right)}{\sum\left(m/\left|c_j\right|\right)}, \tag{7}$$

$$T_{\text{tr,jump}} = \frac{1}{3R}\frac{\sum\left(\left(1/\left|c_j\right|\right)\left\|c\right\|^2\right) - \sum\left(1/\left|c_j\right|\right)U_{\text{slip}}^2}{\sum\left(1/\left|c_j\right|\right)} - T_{\text{tr,wall}}, \tag{8}$$

$$T_{\text{rot,jump}} = \frac{1}{k}\frac{\sum\left(e_{\text{rot}}/\left|c_j\right|\right)}{\sum\left(1/\left|c_j\right|\right)} - T_{\text{rot,wall}}, \tag{9}$$

$$T_{\text{jump}} = \frac{\zeta_{\text{tra}}T_{\text{tra}} + \zeta_{\text{rot}}T_{\text{rot}}}{\zeta_{\text{tra}} + \zeta_{\text{rot}}}. \tag{10}$$

In the preceding equations, U_{slip}, $T_{\text{tra,jump}}$, $T_{\text{rot,jump}}$ and T_{jump} are the slip velocity, and translational, rotational and overall temperature jumps, respectively. $T_{\text{tra,wall}}$ and $T_{\text{rot,wall}}$ are the translational and rotational temperatures of plates. For our cases, $T_{\text{tra,wall}} = T_{\text{wall}}$ and $T_{\text{rot,wall}} = 0.R$ are the ideal gas constants, equal to 208 and 297 ($\text{JKg}^{-1}\text{K}^{-1}$) for argon and nitrogen, respectively. ζ_{tra} and ζ_{rot} are the translational and rotational degrees of freedom and e_{rot} is the rotational energy. The wall shear stress and heat fluxes are defined as below [16]:

$$\tau_w = \frac{F_{num}}{t_s.\Delta A}\sum m(c_i^{inc} - c_i^{\text{ref}}), \tag{11}$$

$$q_w = \frac{F_{num}}{t_s.\Delta A}\left[\sum\left(\frac{1}{2}mc^2\right)^{inc} - \sum\left(\frac{1}{2}mc^2\right)^{\text{ref}}\right]. \tag{12}$$

Here, F_{num} is the number of real molecules that each simulated particle represents, t_s is the sampling time, and ΔA is the interaction area. Superscripts, i and r, denote the incident and reflected particles, respectively.

3.1. Grid study and comparison

To achieve cell independent solutions, we simulate argon flow in a channel using three different grid resolutions in a y direction. We kept the number of particles per cell constant, i.e. an average of 300 particles per cell, and set Knudsen and Mach numbers to 0.2 and 1.05, respectively. Although the problem is one-dimensional, we employed a two-dimensional code and imposed periodic boundary condition on both sides of the domain to correctly simulate infinite length plates. Figure 2 shows the velocity and temperature profiles of argon gas for Grid 1 (150,000 particles in 10×50 cells), Grid 2 (300,000 particles in 10×100 cells) and Grid 3 (450,000 particles in 10×150 cells), respectively. Since flow properties change only in the vertical direction, the effect of cell size in the x direction is not considered. It is observed that Grids 2 and 3

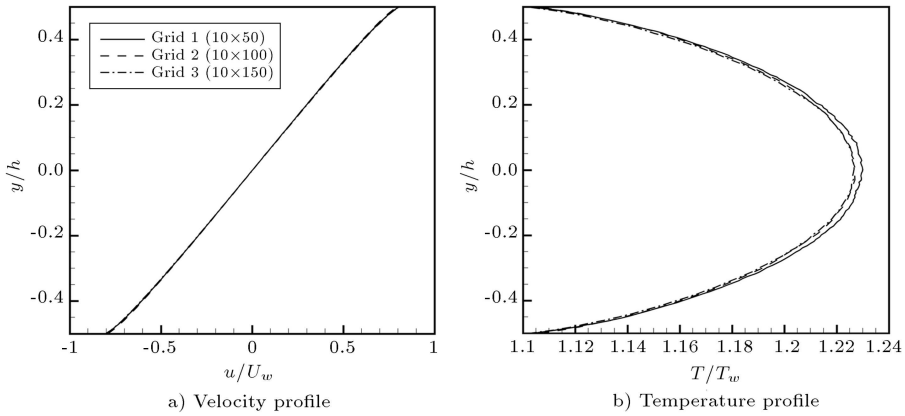

Figure 2. Grid study test: (a) Velocity profile, and (b) temperature profile.

give almost identical velocity and temperature profiles. Therefore, we continue our study using Grid 2.

The approximate Navier-Stokes (NS) solutions for planar Couette flows are available within the framework of continuum fluid mechanics subject to velocity slip and temperature jump boundary conditions, and are valid for the low-velocity (subsonic) flows where variations of density are insignificant in the flow field [1]. Marques et al. [6] showed that the approximate NS solution for the streamwise velocity and the temperature profile in the Couette flow could be written as:

$$U = \frac{U_w}{1 + k_0 \mathrm{Kn}} \frac{2y}{h}, \tag{13}$$

$$T = T_w + \frac{2m}{15k}(1 + 2k_1 \mathrm{Kn})\left(\frac{U_w}{1 + k_0 \mathrm{Kn}}\right)^2 - \frac{2m}{15k}\left(\frac{U_w}{1 + k_0 \mathrm{Kn}}\right)^2 \left(\frac{2y}{h}\right)^2. \tag{14}$$

For hard sphere gases, k_0 and k_1 are two constants with values, 1.111 and 2.127, respectively [24,25]. For a Newtonian, viscous heat-conducting fluid rarefied Couette flow in the early slip regime, the shear stress and the heat flux could be derived using [6]:

$$\tau_{xy} = \mu \frac{U_w}{1 + k_0 \mathrm{Kn}} \frac{2}{h}, \tag{15}$$

$$q_y = \mu \left(\frac{U_w}{1 + k_0 \mathrm{Kn}}\right)^2 \frac{4y}{h^2}. \tag{16}$$

It should be noted that the Marques et al. [6] equation for the velocity profile is not self-consistent, since the velocity slope at the channel center is fitted with the DSMC result. Figure 3(a) compares the DSMC solution for velocity, temperature, non-dimensional heat flux and shear stress with approximate NS solutions given by Eqs. (13) - (16). In this comparison, the Knudsen number is set equal to 0.01 and the wall Mach number is 0.16. At this low Mach number, approximate solutions are quite close to DSMC's. There are some oscillations in the DSMC solutions, which are due to statistical scatter inherent in the DSMC method. The DSMC's statistical scatter decreases with the inverse square root of the sample size. Therefore, a large sample size is required to reduce the scatter. Figure 3(b) compares our DSMC solution with the DSMC solution of Ref. [26], numerical solution of the full NS equations [13] and approximate solutions given by Eqs. (13) and (16). This figure shows that as the

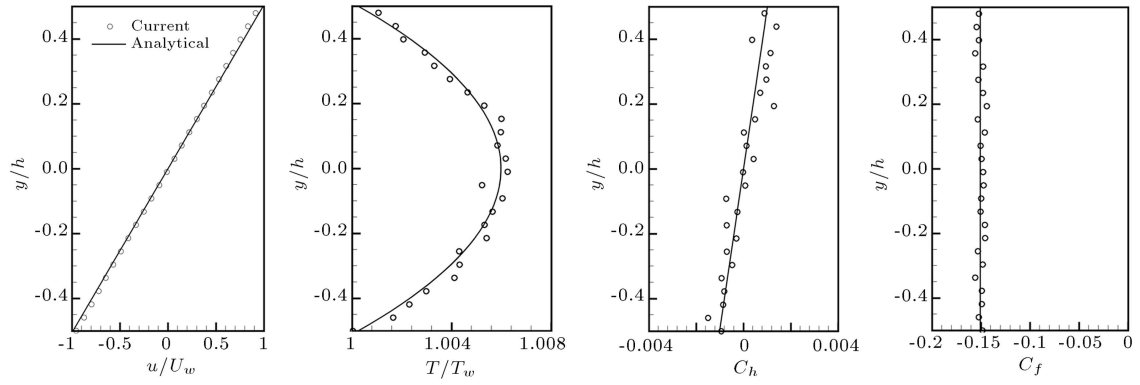

a) Kn=0.01, $M_{\mathrm{wall}} = 0.16$

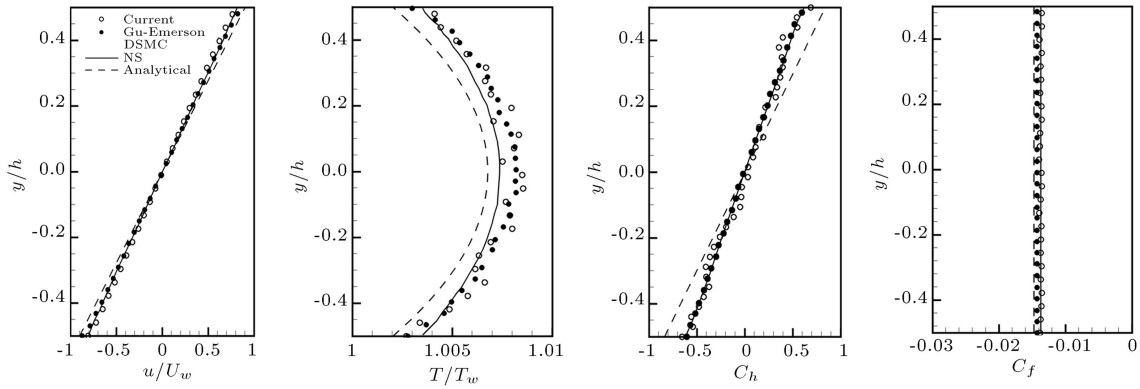

b) Kn=0.1, $M_{\mathrm{wall}} = 0.16$

Figure 3. Comparison of current results with different analytical and numerical solutions.

flow rarifies, approximate solutions deviate from both DSMC solutions. However, numerical NS solutions are closer to DSMC's, which is due to employing more accurate first order velocity slip and temperature jump boundary conditions in the numerical NS code. Our DSMC solution is close to the DSMC solution of Ref. [8], except for larger scatter in our simulation, due to smaller sample size compared with Gu and Emerson simulations [13].

It should be noted that there are alternative analytical formula for the velocity profile of the Couette flow. For example, Lilley and Sader [27] showed that the velocity gradient is singular at the surface and suggested a power law velocity profile in the Knudsen layer for Couette flow. They used a DSMC solution to find a suitable fit parameter for their power formula for a case with Kn=0.006 and $U_{\text{wall}} = 30$ m/s.

3.2. Compressibility effects

The reduction in dimensions of the devices results in the importance of surface effects, due to the increase in surface area. This leads to a dominance of viscous forces over inertial forces. Therefore, variations of pressure and density could be significant, even though the Mach number is well below the conventional limit of 0.3 [28]. The wall Mach number, M_{wall}, is defined as the ratio of U_w to parameter $\sqrt{\gamma k T_w/m}$ and is specified by varying the driving velocity of both plates, U_w. The pressure in linear Couette flow is constant, consequently, compressibility effects are due to the temperature changes only. At first, we performed simulations in such a way that by keeping the Knudsen number constant and varying the Mach number, the compressibility effects are the effective issue. We set the Mach number in such a way that different Mach regimes from subsonic to supersonic are covered. In Figures 4 through 7, velocity, temperature, heat flux and shear stress in domain are plotted for both monatomic argon and diatomic nitrogen gases, for wall Mach numbers changing from 0.2 to 1.2. In Figure 4, the velocity profiles are almost identical to each other. In fact, there are small variations in velocity profiles from low subsonic wall Mach number to early supersonic wall speed, for both gases. However as the normalized velocity, i.e. U/U_w, is plotted in Figure 4, one can conclude that the increments of both the velocity in the domain and the gas velocity slip on the wall are proportional to the increase in wall velocity. Therefore, the ratio of U/U_w is nearly constant for all cases. It is observed that the velocity profile deviates from the linear incompressible velocity profile for the compressible, rarefied gas near the wall. For the range of simulations performed here, the deviation from the linear profile is small, and the maximum deviation occurs for the case of maximum plate velocity. Here, the maximum deviation in the non-dimensional velocities is about 0.008, which is observed near the plates at $M_{\text{wall}} = 1.2$. This is because the macroscopic velocity only depends on the microscopic velocity of the molecules, which is independent of the degree of freedom of molecules. The microscopic velocity is determined according to the amount of kinetic energy transferred from the wall to gas molecules, which increases for higher wall speed values.

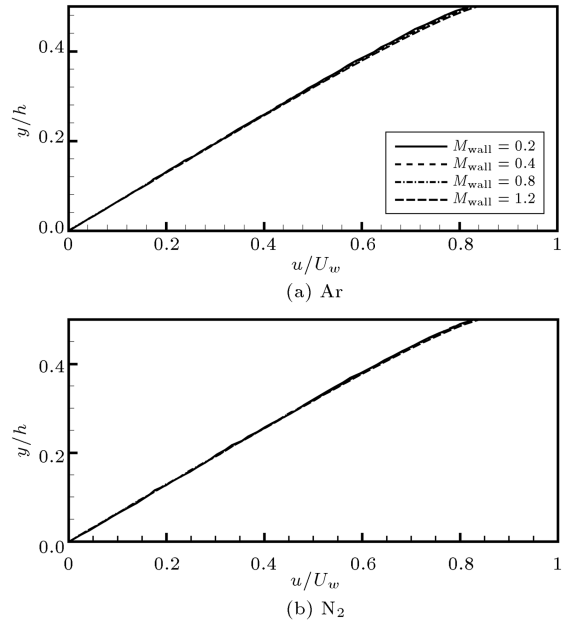

Figure 4. Study of compressibility effects: Velocity profile for different mach numbers; Kn = 0.1, $T_w = 273$ (K).

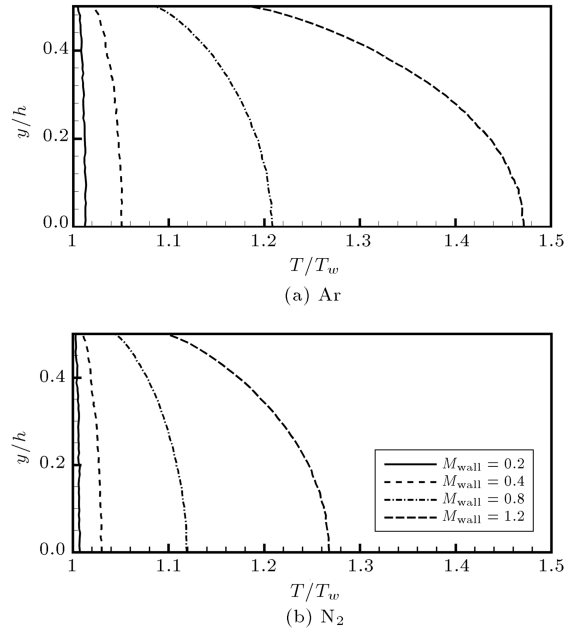

Figure 5. Study of compressibility effects: Temperature profile for different mach numbers; Kn = 0.1, $T_w = 273$ (K).

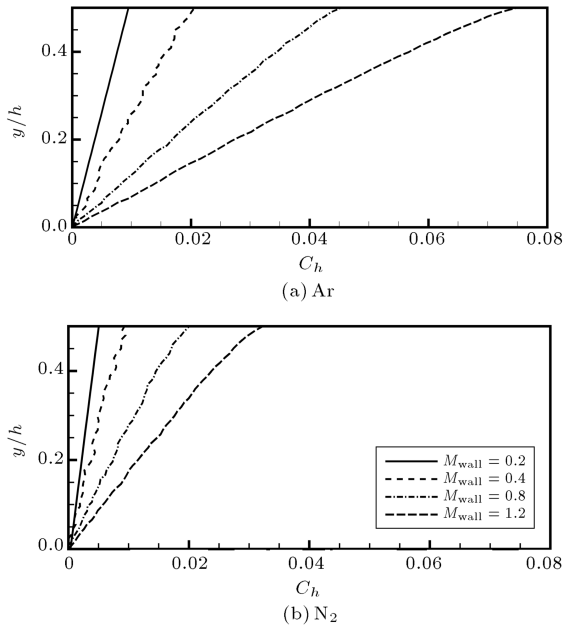

Figure 6. Study of compressibility effects: Heat flux profile for different Mach numbers; Kn = 0.1, $T_w = 273$ (K).

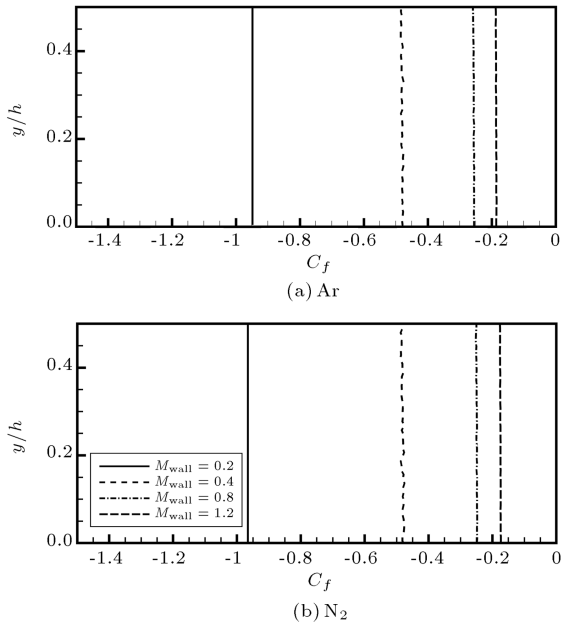

Figure 7. Study of compressibility effects: shear stress profile for different Mach numbers; Kn = 0.1, $T_w = 273$ (K).

Figure 5 shows the variation of temperature in the domain with wall Mach variations. The temperature profiles show that, as M_{wall} increases, the temperature difference between the plates and the center of the channel becomes larger due to higher viscous dissipation. Thus, compressibility effects become significant. The increase of temperature jump at the walls by increasing the Mach number is quite obvious, especially for the monatomic argon gas in Figure 5(a). The magnitude of the temperature jump for argon gas at $M_{\text{wall}} = 1.2$ is almost 47% of the wall temperature. This amount for nitrogen gas at the same Mach number is about 27% of the wall temperature. This decrease of temperature in the domain is explained by an increase in heat capacity, due to using a gas with five degrees of freedom instead of three. The relation between C_p and ζ is given by $C_p = (\zeta/2 + 1)R$. Therefore, as the heat capacity of nitrogen is higher, it has lower temperature compared to the argon for the same Knudsen and Mach numbers. Figure 6 shows the non-dimensional heat flux profile. It shows that the slope of the heat flux profiles increases by increasing the wall Mach number. This is explained by the temperature increase in the domain as a result of viscous heating. By increase of temperature, larger thermal velocities would accelerate the frequency of the momentum exchange between the gas and plates. As a result, higher heat fluxes for higher wall Mach numbers are observed in Figure 6. Comparison of mon/diatomic gases in Figure 6(a) and (b) shows that the magnitude of C_h decreases when dealing with diatomic nitrogen gas. This is also explained by the effect of degrees of freedom on specific heat capacities, as discussed before.

The profiles of normalized shear stress in Figure 7 show the uniform distribution of normalized shear stress in the domain. The figure indicates a decrease in the absolute amount of shear stress by increasing the wall Mach number. This is explained by a decrease in the probability of intermolecular collisions due to a decrease in the total collision cross section (σ_T), according to the relation below [16]:

$$\sigma_T = \sigma_{\text{ref}}\left(\frac{c_r^2}{c_{r,\text{ref}}^2}\right)^{-\alpha}. \tag{17}$$

Here, c_r is the relative velocity of the colliding molecules, $\alpha = 2/(\eta - 1)$, where η is the parameter indicating the hardness of particles and the subscript 'ref' denotes the reference values at the reference temperature, T_{ref}. The values of α for argon and nitrogen for VHS molecules at 273 K are 0.31 and 0.24, respectively [2]. As Mach number increases, the relative velocity of the molecules in the domain would increase. Therefore, the total collision cross section, and the probability of intermolecular collisions decreases. Consequently, higher wall Mach numbers would lead to smaller magnitudes of shear stress. From the macroscopic point of view, the classical relationship between three basic non-dimensional numbers, Mach, Reynolds and Knudsen, is given by:

$$\text{Kn} = \frac{\text{Ma}}{\text{Re}}\sqrt{\frac{\gamma\pi}{2}}. \tag{18}$$

In a constant Knudsen number, as Mach number increases, the Reynolds number would increase. The

increase of Reynolds number means the dominance of the inertial forces over the viscous forces. Therefore, due to the convective nature of the flow, the effect of molecular diffusion gets smaller and less magnitudes of C_f are observed. Comparing Figure 7(a) and (b), it is observed that the magnitude of C_f is almost the same for monatomic and diatomic gases for Kn=0.1. However, as will be discussed later, the magnitude of non-dimensional shear stress increases for diatomic gas in comparison with the monatomic gas for lager Knudsen numbers.

3.3. Rarefaction effects

Rarefaction effects gain importance with the reduction in the geometry size, since the sizes of the geometries become comparable to the mean free path of the gas molecules. These effects are specified through the Knudsen number. Now, the plates' velocity is kept constant ($U_w = 250$ m/s) and the corresponding wall Mach numbers are 0.81 and 0.74 for argon and nitrogen, respectively. This difference in the wall Mach number is due to the different specific heat ratio (γ) of two gases. Figure 8 shows normalized velocity profiles. This figure considers rarefaction effects for six different Knudsen numbers in the entire Knudsen regimes, i.e. from continuum to free molecular. We simulate Knudsen numbers corresponding to the early and end parts of the slip regime (Kn = 0.01 and 0.1), and early, mid, and end parts of the transition regime (Kn = 0.5, 1, 5 and 10). It is observed in Figure 8, that the slope of the velocity profile decreases as Knudsen number increases. This means a decrease of velocity in the domain. In a constant wall Mach number flow, as

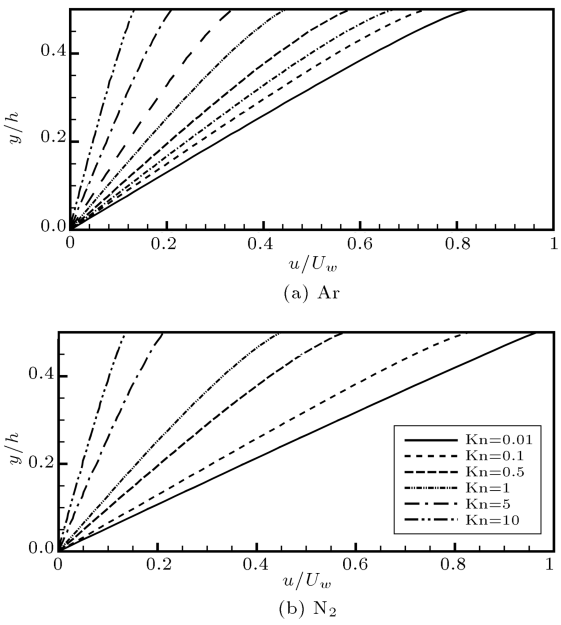

Figure 8. Study of rarefaction effects: velocity profile for different Kn number flows; $U_w = 250$ (m/s), $T_w = 273$ (K).

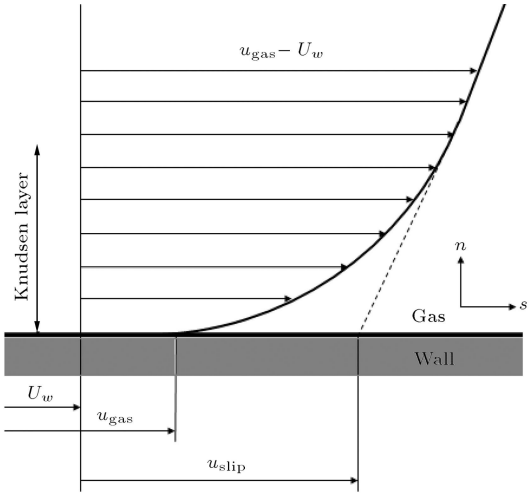

Figure 9. Schematic diagram showing Knudsen layer and slip velocity.

the flow becomes rarefied, the number of molecules colliding into the moving walls and transferring the kinetic momentum from the moving wall to the domain decreases. Therefore, the velocity in the domain decreases as the Knudsen number increases. Analytical solution of the linearized Boltzmann equation indicates that the bulk flow velocity profile is essentially linear for all Knudsen numbers [1]. However, a kinetic boundary layer, named Knudsen layer, on the order of one to a few mean free paths, starts to become dominant between the bulk flow and solid surfaces in the transition flow regime [29,30]. Figure 9 is a schematic diagram showing the Knudsen layer. In the figure, u_{gas} is the real slip velocity of the gas inside the Knudsen layer, and u_{slip} is the approximate value obtained from the NS equations to calculate the velocity profile in the entire flow field. As observed in Figure 8, when Kn=0.01, the velocity profile is linear, but when Kn>0.1, the linear velocity profiles no longer exist. This is due to the increase of the thickness of the Knudsen layer in the transition flow regime. Gallis et al. [31] reported that within the Knudsen layer, molecules collide with the surface more frequently than they collide with each other. As a result, when Knudsen number is small (Kn<0.1), the change of velocity in the Knudsen layer is negligible in the entire velocity profile; however, in the slip and transition flow regimes, Knudsen layer occupies a significant proportion of the channel in the Couette problem, and a non-Newtonian behavior becomes pronounced. In Figure 8, it is observed that bending in the velocity profile occurs most specifically at Knudsen number equal to 1. However, with further increase in Knudsen number, the velocity profiles are tending to the linear profiles again. This is because the flow will enter the free molecular regime, where the Knudsen layer occupies the domain completely. These observations quite conform with the results reported by

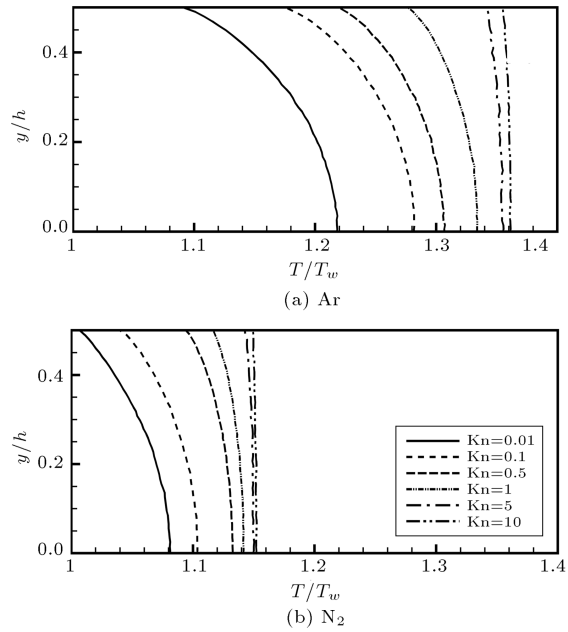

Figure 10. Study of rarefaction effects: Temperature profile for different Kn number flows; $U_w = 250$ (m/s), $T_w = 273$ (K).

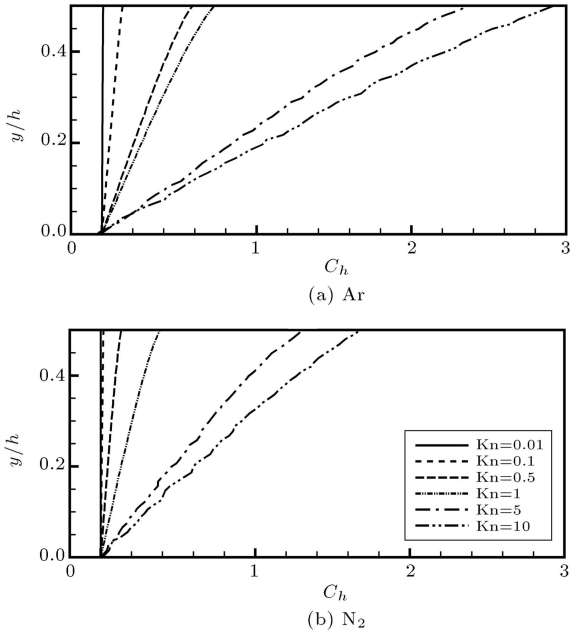

Figure 11. Study of rarefaction effects: Heat flux profile for different Kn number flows; $U_w = 250$ (m/s), $T_w = 273$ (K).

Xue et al. [8]. It is also observed that by increasing the Knudsen number, the slip velocity increases. It should be noted that the slip velocity at the plates would reach its maximum value as the Knudsen number approaches 10. It is also observed, in Figure 8(a) and (b), that using diatomic gas instead of monatomic gas has almost no effect on the bulk velocity of the domain. Here, the maximum deviation in the velocity profiles is about 0.005 at Kn=1.

Figure 10 illustrates the temperature profiles at different Knudsen numbers. As the Knudsen number increases, temperature in the domain and also the temperature jump at the plates becomes more significant, but the curvature of the temperature profiles reduces. In a constant wall Mach number flow, the amount of wall kinetic energy is constant. As the flow becomes more rarefied, this constant kinetic energy will be saved in a smaller number of molecules, and shows itself in terms of temperature rise. However, in a dense gas, this amount of constant energy is distributed in a larger number of molecules, and the temperature rise is smaller than that observed in rarefied gases. Also for small Knudsen numbers and close to the continuum regime, only near surface molecules collide with the walls, and only in the middle of the channel do intermolecular collisions happen. For larger Knudsen numbers, as the gas becomes more rarefied, molecules in the middle of the channel have the same chance for molecular-surface collision and transferring heat with the walls. Consequently, the maximum curvature in Figure 10 is observed in the Kn=0.01, and, by increase in Knudsen number, the temperature in the domain becomes uniform. The maximum temperature in the center of the channel for nitrogen is about 95% of the maximum temperature for argon, when Kn = 0.01. This fraction is about 85%, when Kn = 10. This means that the effect of mon/diatomic structures will be more significant in rarefied conditions.

Figure 11 shows the non-dimensional heat flux variation. It is observed that, by increasing the Knudsen number, the magnitude of heat flux in the domain increases. This is because of an increase in the surface-molecular collisions, due to an increase in the mean free path of the molecules. As a result, not only can the molecules near the surface, but also the molecules at the center of the channel, collide with the surfaces. Therefore, more absorbed kinetic energy from the wall is transferred into heat. The increase in the slope of the non-dimensional heat flux for Kn>5 slows down, which is an absolute result of rarefaction effects. It is also observed in Figure 11(a) and (b) that the diatomic gases experience a lower amount of heat flux than monatomic ones. The reasoning is similar to that already discussed for Figure 6.

Our simulations show that, as the gas becomes more rarefied, it will experience less shear stress due to a smaller amount of intermolecular collisions. However, the magnitude of non-dimensional shear stress would still increase, as observed in Figure 12. In other words, as shear stress is normalized by the term, including free stream density, ρ_∞, it is correct to say that by increasing the Knudsen number, the magnitude of normalized shear stress increases, even though the magnitude of shear stress decreases. It is observed that, in Eq. (18),

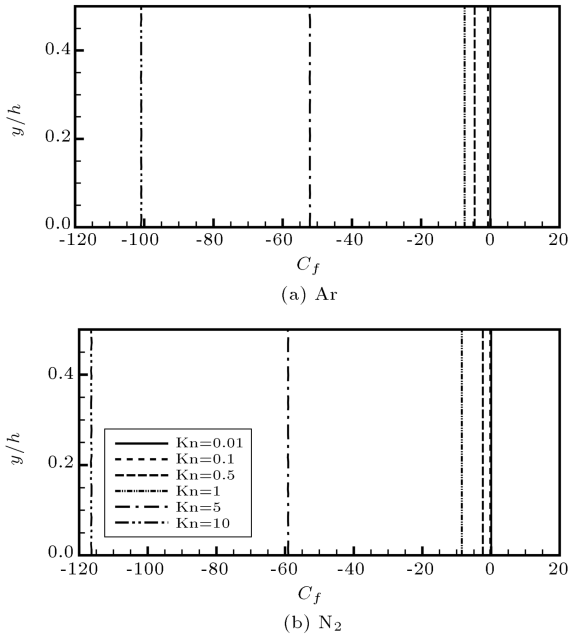

Figure 12. Study of rarefaction effects: Shear stress profile for different Kn number flows; $U_w = 250$ (m/s), $T_w = 273$ (K).

by increasing the Knudsen number, Reynolds number would decrease. This means the dominance of viscous forces over inertial forces at higher Knudsen number flows. As viscosity increases, temperature, heat flux and shear stress would increase, which totally supports molecular or microscopic theories. Comparison of Figure 12(a) and (b) shows that the shear coefficient for monatomic and diatomic gases is almost the same when Kn=0.01. But the difference in the magnitude of shear stress coefficients becomes larger in rarefied gases.

Figures 13 and 14 show the variations of different properties, such as velocity slip, temperature jump, wall heat and shear stress, on the surface. Here, our purpose is to compare mon/diatomic gas behaviors, study Kn number effects and compare the values sampled directly from Eqs. (7) through (12) with the macroscopic (volume based) values of these properties calculated in the adjacent cells near the wall. Figure 13 shows that the velocity slip and temperature jump increase as Knudsen number increases, however, the rate of this increase slows down as the flow approaches the free molecular regime. Both the direct sampling method and volume based method are in agreement with each other for Couette flow. In fact, if flow does not experience large gradients on the surface cells, volume-based sampling would provide solutions close to direct sampling solutions. Figure 14 shows that the wall heat flux and absolute amount of wall shear decreases by an increase in Knudsen number. Both volume based and microscopic methods show the same trend. There is small difference between the values predicted by both methods, while it is expected that the direct sampling method will provide the accurate solution.

We have plotted the probability density function (PDF) for a cell in the middle of the geometry in Figure 15(a) and (b). This is a particular location, because the velocity of molecules above this location would have a net velocity in the direction of the upper plate, and the molecules below there would have a velocity in the reverse direction. We also plotted the Maxwellian equilibrium distribution in that figure to investigate the deviation from equilibrium [2]. Maxwellian distribution describes the probability of finding a randomly selected particle in a unit volume element in the velocity space for equilibrium gases, and is given by [16]:

$$f_0 = (\frac{m}{2\pi kT})^{3/2} \exp(-\frac{m\mathbf{c}'^2}{2kT}). \quad (19)$$

PDF shown in Figure 15(a) illustrates that by increas-

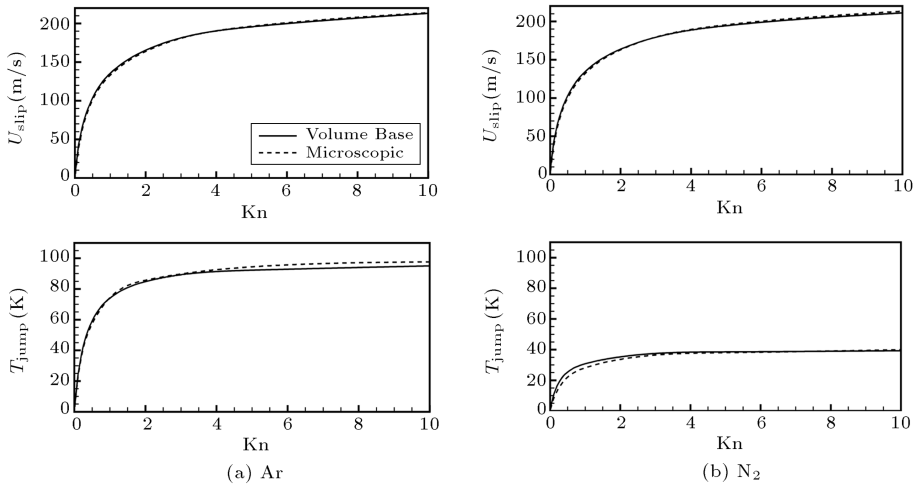

Figure 13. Comparison of volume-based-results with microscopic results.

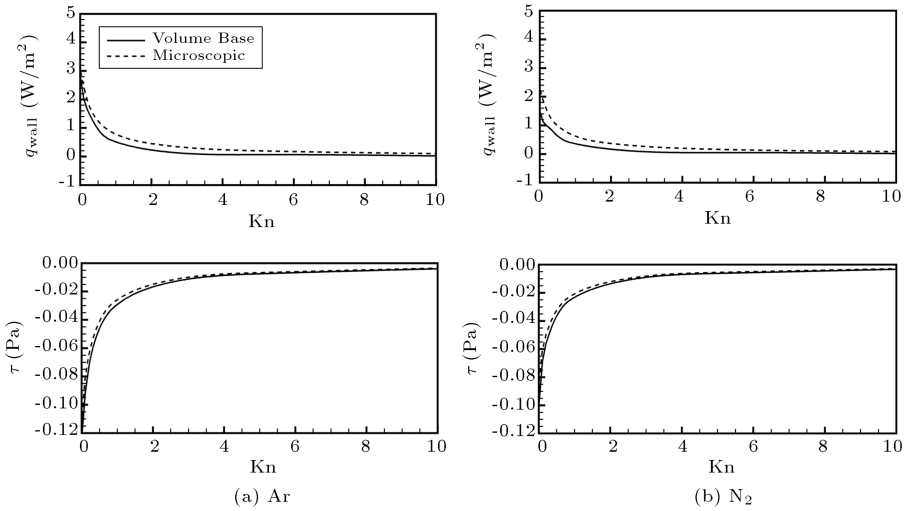

Figure 14. Comparison of volume-based-results with microscopic results.

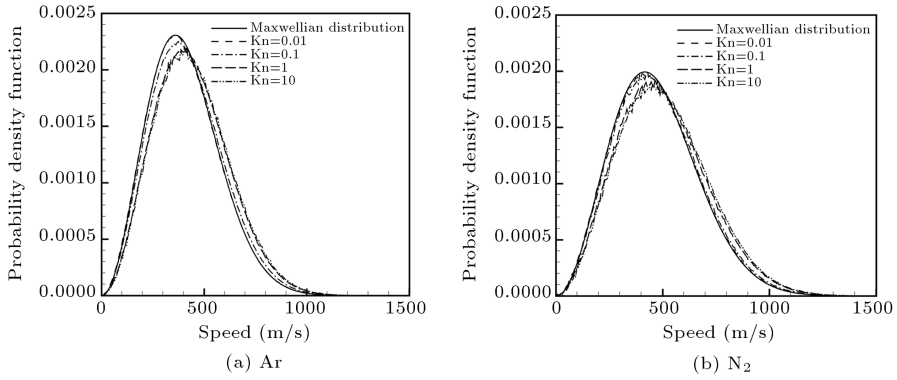

Figure 15. Study of rarefaction effects: Probability density function for different Kn number flows; $U_w = 250$ (m/s), $T_w = 273$ (K).

ing the Knudsen number, the flow deviates from the equilibrium more. It is observed in Figure 15(a) that all curves have a global maximum. By increasing the Knudsen number, this global maximum deviates from its identical point in the Maxwellian distribution. Also, the curves shift to the right when the Knudsen number increases. It is observed that when Kn=0.01, the curve is almost identical to Maxwellian distribution, and the maximum deviation occurs when Kn=10. Figure 15(b) illustrates a similar distribution with almost 15% decrease in the magnitude of the global maximum for diatomic nitrogen gas. This is due to the lower mass of nitrogen compared to argon. However, nitrogen molecules have greater PDF for higher velocity magnitudes.

4. Conclusion

We studied nano/micro Couette flow through a channel for a wide range of Mach and Knudsen numbers, using the DSMC method. We investigated compressibility and rarefaction effects on the behaviors of velocity, temperature, heat flux and shear stress profiles for monatomic argon and diatomic nitrogen gases. Compressibility tests showed that an increase in wall velocity results in an increase in non-dimensional velocity, temperature and heat flux, but a decrease in the magnitude of shear stress in the domain. The most important parameter here was the viscous dissipation, which increased as the wall velocity increased and caused a temperature increase in the domain. Rarefaction tests showed that an increase in Knudsen number results in a decrease in non-dimensional velocity, but an increase in temperature, an absolute amount of non-dimensional heat flux and shear stress in the domain. It is observed that the gradient of the velocity profiles decreases as the flow becomes more rarefied. It is also observed that when Kn=0.01, the velocity profile is linear, but, by increasing the Knudsen number, the velocity profile deviated from the linear profiles and a non-Newtonian behavior was observed. This is due to the increase in the thickness of the Knudsen layer in the transition flow regime. Comparison of surface parameters calculated by both microscopic and volume based macroscopic methods showed good agreement between these two methods in prediction of slip velocity and temperature

jump. However, slight deviations were observed in the prediction of wall heat flux and shear stress at small Knudsen numbers. All surface properties approached a nearly constant value as the flow approached the free molecular regime. While the velocity slips of both monatomic and diatomic gases were the same, the latter had a much smaller temperature jump. This is due to the higher heat capacity of the diatomic nitrogen. We also illustrated deviation from the equilibrium by plotting the probability density function in a particular cell. Nitrogen gas had a lower global maximum in PDF due to lower mass, while it has more molecules with higher velocity magnitudes.

References

1. Karniadakis, G., Beskok, A. and Aluru, N., *Micro Flows and Nano Flows: Fundamentals and Simulation*, New York: Springer-Verlag (2005).
2. Bird, G.A., *Molecular Gas Dynamics and the Direct Simulation of Gas Flows*, Clarendon Press, Oxford, United Kingdom (1994).
3. Willis, D. "Comparison of kinetic theory analyses of linearized Couette flow", *Phys. Fluids,* **5**(2), p. 127 (1962).
4. Sirovich, L. "Approximate method in kinetic theory. Couette flow and the Kramers problem", *Phys. Fluids,* **12**(3), pp. 586 (1969).
5. Beskok, A., Karniadakis, G.E. and Trimmer, W. "Rarefaction and compressibility effects in gas microflows", *J. of Fluids Eng.*, **118**(3), pp. 448-456 (1996).
6. Marques Jr, W., Kremer, G.M. and Sharipov, F.M. "Couette flow with slip and jump boundary conditions", *Continuum Mech. and Thermodynamics*, **12**(6), pp. 379-386 (2000).
7. Xue, H., Fan, Q. and Shu, C. "Prediction of microchannel flows using direct simulation Monte Carlo", *Probabilistic Eng. Mech.*, **15**(2), pp. 213-219 (2000).
8. Xue, H., Ji, H.M. and Shu, C. "Analysis of micro-Couette flow using the Burnett equations", *Int. J. of Heat and Mass Transfer*, **44**(21), pp. 4139-4146 (2001).
9. Xue, H. and Ji, H. "Prediction of flow and heat transfer characteristics in micro-Couette flow", *Microscale Nanoscale Thermophysical Eng.*, **7**(1), pp. 51-68 (2003).
10. Frezzotti, A. and Gibelli, L. "A kinetic model for fluid-wall interaction", *Proccedings of the Institution of Mech. Eng., Part C: J. of Mech. Eng. Scie.*, **222**(5), pp. 787-795 (2008).
11. Frezzotti, A., Nedea, S.V., Markvoort, A.J. et al. "Comparison of molecular dynamics and kinetic modeling of gas-surface interaction", *AIP Conference Proceedings,* **1084**(1), pp. 635-640 (2008).
12. Frezzotti, A., Gibelli, L. and Franzelli, B. "A moment method for low speed microflows", *Continuum Mech. and Thermodynamics*, **21**(6), pp. 495-509 (2009).
13. Gu, X.J. and Emerson, D.R. "A high-order moment approach for capturing non-equilibrium phenomena in the transition regime", *J. of Fluid Mech.*, **636**, pp. 177-216 (2009).
14. Kumar, R., Titov, E. and Levin, D. "Reconsideration of planar Couette flows using the statistical Bhatnagar-Gross-Krook approach", *J. of Thermophysics and Heat Transfer*, **24**, pp. 9 (2010).
15. Meng, J. and Zhang, Y. "Analytical solutions for the lattice boltzmann model beyond naviers-stokes," *Adv. Appl. Math. Mech.*, **2**(5), pp. 670-676 (2010).
16. Liou, W.W. and Fang, Y., *Microfluid Mechanics: Principles and Modeling*, McGraw-Hill (2006).
17. Cercignani, C., *Rarefied Gas Dynamics. From Basic Concepts to Actual Calculations*, Cambridge University Press (2000).
18. Roohi, E. and Darbandi, M. "Extending the navier-stokes solutions to transition regime in two-dimensional micro- and nanochannel flows using information preservation scheme", *Physics of Fluids*, **21**(8), p. 082001 (2009).
19. Scanlon, T.J., Roohi, E., White, C. et al. "An open source, parallel DSMC code for rarefied gas flows in arbitrary geometries", *Computers & Fluids*, **39**(10), pp. 2078-2089 (2010).
20. Darbandi, M. and Roohi, E. "Study of subsonic—supersonic gas flow through micro/nanoscale nozzles using unstructured DSMC solver", *Microfluidics and Nanofluidics*, **10**(2), pp. 321-335 (2011).
21. Ejtehadi, O. Roohi, E. and Esfahani, J.A. "Investigation of basic molecular gas structure effects on hydrodynamics and thermal behaviors of rarefied shear driven flow using DSMC", *Int. Communications in Heat and Mass Transfer,* **39**(3), pp. 439-448 (2012).
22. Esfahani, J.A., Ejtehadi, O. and Roohi, E. "Second law analysis of micro/nano Couette flow using direct simulation Monte Carlo method", *Int. J. of Exergy*, in press (2013).
23. Lofthouse, A.J., *Nonequilibrium Hypersonic Aerothermodynamics Using the Direct Simulation Monte Carlo and Navier-Stokes Models*, University of Michigan (2008).
24. Loyalka, S. and Hickey, K. "Velocity slip and defect: Hard sphere gas", *Phys. Fluids A,* **1**(3), pp. 612 (1989).
25. Sone, Y., Ohwada, T. and Aoki, K. "Temperature jump and Knudsen layer in a rarefied gas over a plane wall: Numerical analysis of the linearized Boltzmann equation for hard sphere molecules", *Phys. Fluids A*, **1**(2), pp. 363 (1989).
26. Gillan, M.J. and Dixon, M. "The calculation of thermal conductivities by perturbed molecular dynamics simulation", *J. of Physics C: Solid State Physics*, **16**(5), pp. 869 (1983).
27. Lilley, C. and Sader, J. "Velocity gradient singularity and structure of the velocity profile in the Knudsen layer according to the Boltzmann equation", *Physical*

Review E (Statistical, Nonlinear, and Soft Matter Physics), **76**(2), pp. 026315 (2007).

28. Gad-el-Hak, M. "The fluid mechanics of microdevices-the freeman scholar lecture", *J. of Fluids Eng.*, **121**(1), pp. 5-33 (1999).

29. Cercignani, C., *Mathematical Methods in Kinetic Theory*, Plenum Press, New York (1990).

30. Sone, Y., *Kinetic Theory and Fluid Dynamics*, Boston, Birkhauser (2002).

31. Gallis, M.A., Torczynski, J.R., Rader, D.J. et al. "Normal solutions of the Boltzmann equation for highly nonequilibrium Fourier flow and Couette flow", *Physics of Fluids*, **18**(1), p. 017104 (2006).

Biographies

Omid Ejtehadi obtained an MS degree from Ferdowsi University of Mashhad, Iran, in 2012. His research interests include: rarefied gas dynamics, DSMC simulation of micro/nano flows, and MEMS/NEMS. To date, he has published 3 journal papers and 4 conference papers.

Ehsan Roohi obtained a PhD degree in Aerospace Engineering from Sharif University of Technology, Tehran, Iran, in 2010, and is currently Assistant Professor of Mechanical Engineering at Ferdowsi University of Mashhad, Iran. To date, he has published 28 journal articles and 38 conference papers. His research interests include: rarefied gas dynamics, Direct Simulation Monte Carlo (DSMC) and two phase flows.

Javad Abolfazli Esfahani obtained a PhD degree in Mechanical Engineering from the University of New Brunswick (UNB), Canada, in 1997, and is currently Professor of Mechanical Engineering at Ferdowsi University of Mashhad, Iran. To date, he has published 5 books/chapters, 52 journal articles and more than 80 conference papers. Dr. Esfahani is a member of Centers of Excellence in Energy Conversion (CEEC), on Modelling and Control Systems, (CEMCS) and in Energy Management (CEEM). He is also a member of the Iranian Combustion Institute and the Iranian Society of Mechanical Engineering, and is also on the Editorial Boards of the Journal of Fuel and Combustion (Iranian) and IRECHE. His research interests include: theoretical and numerical heat and mass transfer.